Effect of Oxygen on the Crosslinking and Mechanical Properties of a Thermoset Formed by Free-Radical Photocuring

Morgan Pilkenton,[1] Jeremiah Lewman,[1] Richard Chartoff[1,2]

[1]*Department of Chemical and Materials Engineering, University of Dayton, Dayton, Ohio 45469-0246*
[2]*Materials Science Institute, Department of Chemistry, University of Oregon, Eugene, Oregon 97403*

Received 23 October 2009; accepted 15 April 2010
DOI 10.1002/app.32650
Published online 1 September 2010 in Wiley Online Library (wileyonlinelibrary.com).

ABSTRACT: In this article, we report on the formation of optically transparent photopolymer films from hexanediol diacrylate (HDDA) by inkjet printing, where droplets of monomer approximately 5 μm in diameter were deposited onto a surface. The films were cured by irradiation with a UV-light-emitting-diode light source. It was found that the inkjet-printed HDDA films picked up a considerable amount of absorbed O_2 during printing. Exposure to increasing amounts of O_2 during photocuring severely restricted both the degree of conversion and the UV dose required for gelation in proportion to the O_2 concentration. Viscoelastic property data indicated that exposure to reduced oxygen concentrations during thermal postcuring (dark reaction) resulted in linear trends of increasing modulus above the glass-transition temperature (T_g) and increasing T_g itself. Thus, the final crosslink density was greater in fully cured samples that were exposed to atmospheres with increasing inert gas concentrations. © 2010 Wiley Periodicals, Inc. J Appl Polym Sci 119: 2359–2370, 2011

Key words: crosslinking; kinetics (polym.); photopolymerization; viscoelastic properties

INTRODUCTION

Effects of oxygen on free-radical crosslinking reactions

Crosslinked polymers formed by UV photocuring are a class of thermosets whose reaction and thermal characteristics can be characterized by thermal analysis methods, particularly, differential scanning calorimetry (DSC) and dynamic mechanical analysis (DMA). Commonly, photopolymers are applied as films or surface coatings. They are most often formed from the reaction of multifunctional, unsaturated acrylate or methacrylate monomers by a free-radical mechanism. The reactions are facilitated by soluble photoinitiators added in small amounts to the monomers. The photoinitiators are light-sensitive compounds that decompose on irradiation to generate free radicals, which then initiate the polymerization. The initiating radicals combine with available monomers to form primary radicals that, subsequently, propagate through additional monomer units to create a three-dimensional polymer network.[1–3]

Molecular oxygen is known to inhibit free-radical polymerization by reacting with the initiator and primary and growing polymer radicals to form peroxy radicals.[4–8] The peroxy radicals are more stable and do not readily reinitiate polymerization; the oxygen essentially terminates or consumes the radicals. This can occur at several steps in the reaction sequence. Thus, O_2 restricts the degree of conversion, modifies the kinetic chain length, and thus, reduces the amount of crosslinking in the network. Absorbed oxygen may have an effect that in some respects may be likened to that of a chain-transfer agent. The effect of the kinetic chain length on the mechanical relaxation of crosslinked photopolymers was discussed in another publication in the context of chain-transfer agents.[9] It was hypothesized that the addition of a chain-transfer agent to a free-radical crosslinking system would decrease the kinetic chain length and lead to a more mobile reaction environment, more rapid termination rates, and a more open network because of a larger population of dangling chain ends.[10,11] Thus, another consequence of oxygen inhibition is that dissolved O_2 markedly increases the gelation dose, the amount of radiation required to cause gelation. In this study, we examined the influence of these factors on conversion.

If oxygen is present, an induction time will be observed because the polymerization cannot proceed until the propagation reaction competes with the inhibition reaction. Because the equilibrium dissolved oxygen concentration in acrylates is about 10^{-3} M[9,12] and Decker and coworkers[4–6] reported that the oxygen concentration below which polymerization proceeds is about 4×10^{-6} M, the oxygen concentration must drop by a factor of at least 300 before polymerization begins. In thicker films, the lower depths of the film may polymerize, whereas the top layer remains tacky

Correspondence to: R. Chartoff (rchartoff@msn.com).

because oxygen inhibits the surface reaction. At high concentrations or in very thin films, however, oxygen scavenges all of the radicals generated and, thus, inhibits or severely retards the polymerization. Oxygen inhibition in thin films is most important because oxygen readily diffuses back into the sample from the surroundings. This should be exacerbated in inkjet printing, where very small droplets come in contact with air as they are ejected from the inkjet nozzle. In any case, an unpolymerized top layer reduces the film surface quality and optical properties.[9,12,13]

Previous research on oxygen inhibition in crosslinking

Past research has documented the effect of oxygen and has primarily focused on the polymerization rate and developing kinetic models that simulate specific effects that oxygen has on photopolymerization kinetics.[13–17] Nunes and coworkers[18,19] used spatially resolved magnetic resonance imaging to investigate the anisotropic effects of oxygen on the photopolymerization of dental materials. Additionally, Chong[20] and Krongauz et al.[8] developed kinetic models that simulate specific effects that oxygen has on photopolymerization kinetics. Dickey et al.[21] implemented a kinetic model to study the effect of diffusing oxygen at the etch barrier in step and flash imprint lithography. Brady and Halloran,[22] using photo-DSC, showed that oxygen inhibition significantly suppresses the rate of polymerization and monomer conversion of air-irradiated ceramic suspensions in hexanediol diacrylate (HDDA).

Espanet et al.[23] documented how dissolved oxygen in films affects the radiation dose required to achieve gelation. When the monomer contains oxygen, the gel dose increases with increasing exposure to O_2. They also concluded that when the film surface is blocked so it is not in contact with the atmosphere, the competition between the photoreaction and inhibition involves O_2 molecules already present diffusing to reaction sites through the solution. This is likely to be a particular problem in the case of inkjet-deposited films, where large amounts of O_2 may be absorbed by the tiny droplets because, as they are ejected from the inkjet nozzles, the droplets have a large surface-to-volume ratio. O_2 will, thus, be incorporated into the films by entrapment.

The mechanism of the reaction of O_2 with growing polymer radicals and the role of the diffusion of O_2 in polymer film formation has been discussed in detail elsewhere.[24,25] In particular, Andrzejewska et al.[24] considered the kinetics in the presence of oxygen of both crosslinking photopolymerization and the postirradiation dark reaction. They reached the intriguing conclusion that the postpolymerization dark reaction is even more sensitive to retardation by oxygen than is the polymerization under continuous irradiation.

O'Brien and Bowman[26] studied several key factors that affect the extent of oxygen inhibition on photopolymerization kinetics during film formation. Their films were prepared by casting onto flat surfaces. The effects of the sample thickness, ambient oxygen concentration, initial dissolved oxygen concentration, and initiation rate were investigated and modeled. Furthermore, they considered the effect of the initial dissolved oxygen concentration on selected bulk polymer mechanical properties, as determined by DMA. The properties cited were the glass-transition temperature (T_g) and storage modulus at 25°C (which was below T_g). Before this study, it was thought that the effect of dissolved oxygen on the bulk mechanical properties would be to lower the crosslinking density and modulus of the polymer,[8] but this had not been experimentally confirmed. On the sole basis of data for the 25°C storage modulus and glass transition defined by the peak loss tangent (tan δ) value, O'Brien and Bowman[26] did not find a statistical difference in the mechanical properties cited for films exposed to argon (0% O_2) compared to films exposed to air (21% O_2) during their formation. However, to form conclusions about crosslinking effects with DMA viscoelastic property data, it is most desirable to examine modulus values above T_g in the plateau region, where the major effects of crosslinking are normally exhibited. We did that in this study.

Dark reaction after the initial light exposure

After exposure to light, photopolymers usually are only partially reacted, with a degree of conversion of less than 100%. This is similar to what occurs in the case of conventional thermosets. The photopolymerization reactions proceed until gelation and vitrification halt further reaction because of diffusion limitations. The polymer formed on initial radiation exposure is heterogeneous[27–31] with more than one phase present, even when only one monomer is involved. Because of this heterogeneity, they have unusually broad glass transitions. DSC[32–35] and DMA[27,36] data in the literature for reactive multifunctional acrylate monomers show that two major phases are present in partially cured photopolymers.

In a single-component system, such as HDDA, the phase heterogeneity results entirely from the statistical nature of the chain polymerization process, the random coil conformation of the growing chains, and the increased reactivity of dangling, unreacted acrylate groups from monomer units already attached to the network.[27,28] This is consistent with the percolation model forwarded by Kloosterboer and coworkers.[28–31] Their model indicates that for a single monomer (HDDA), both low- and high-crosslink density regions develop, even at low conversions. The high-density phase consists largely of fairly rigid crosslinked materials, and the low-density phase is monomer swollen

gel. Thus, the high-density phase has a high-temperature glass transition, whereas the low-density phase has a lower temperature glass transition. The low-density phase is expected to be quite sensitive to the absorption of oxygen.[26] The amount of the high-density phase increases as the polymerization proceeds, at the expense of the low density phase. The major DMA loss dispersion for the high-temperature phase covers an unusually wide temperature range; this indicates that the crosslink network is quite microheterogeneous. Additional information on phase heterogeneity during cure in such systems has been cited in other publications.[25,27] A comprehensive model for microheterogeneity in thermosets formed by free-radical polymerization from multifunctional monomers, such as HDDA, was detailed in a recent monograph by Korolev and Mogilevich.[25]

Related to this is the fact that when a free-radical photopolymerization is retarded by gelation and vitrification, trapped free radicals are left suspended in the crosslink network.[28,29] The trapped free radicals are free to continue reacting in the dark with unreacted acrylate groups attached to the network or with available residual monomer when the partially cured polymer is heated to temperatures above its glass transition. These and other salient aspects of free-radical photopolymer formation have been reviewed in the literature.[27–31] Thus, the continuation of conversion occurs as the polymer is heated during variable-temperature DSC and DMA scans. The sensitivity to absorbed oxygen at this stage of the reaction and its influence on the nature of the crosslinking reaction is a second issue considered in this article. In the following narrative, we describe our results and conclusions concerning the role of oxygen in the progress of postcuring or the dark reaction phase of the reaction.

Controlling oxygen inhibition

Different techniques have been used to combat the effects of oxygen inhibition and to control its inhibitory effects.[26] The method we have been working with is the polymerization of samples in an inert environment, whereby oxygen is eliminated from the polymerization.[9,33–35] Our objective was to determine the conditions necessary to achieve the highest degree of curing and crosslinking during film processing. Thus, we considered the effect of O_2 on the conversion of the monomer to polymer, the inert gas purge time required to eliminate the effects of O_2, the viscoelastic properties of inkjet-printed films formed in an inert atmosphere and in air, and the change in properties that occurs during the DMA characterization of printed films in contact with various O_2 concentrations. The results presented subsequently are indicative of our findings.

EXPERIMENTAL

Materials

All monomer samples were prepared by the mixture of HDDA with photoinitiators: 1 wt % Irgacure 184 (1-hydroxyl cyclohexyl phenyl ketone) and 0.5 wt % Irgacure 819 [bis(2,4,6-trimethyl benzoyl)–phenylphosphineoxide] in HDDA. The mixtures are referred to simply either as monomer or HDDA in subsequent sections of this article. High-purity HDDA was supplied by Cytec Surface Specialties, Inc., Radcure Division. The photoinitiators were supplied by Ciba Specialty Chemicals, Coating Effects Business Segment. Irgacure 184 was the primary photoinitiator. Irgacure 819 was introduced as a coinitiator because it was particularly useful for promoting through the thickness curing of the films, which were both thick and contained fillers. The photoinitiator amounts were selected (on the basis of experimental determinations) to maximize the photoreaction conversion efficiency:

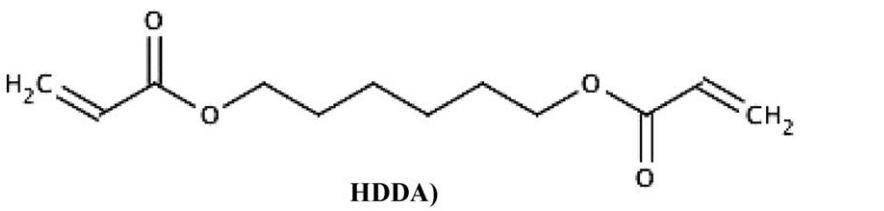

HDDA)

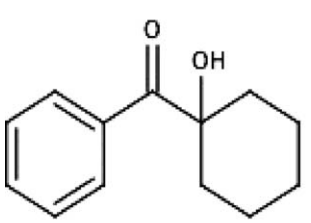

Irgacure 184

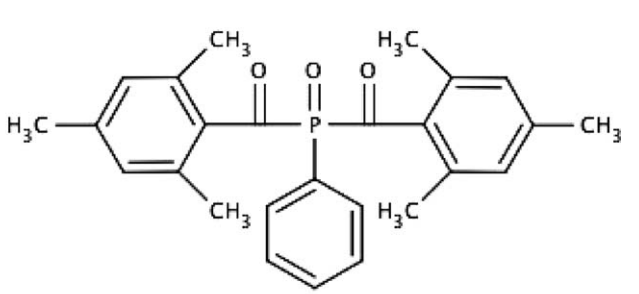

Irgacure 819

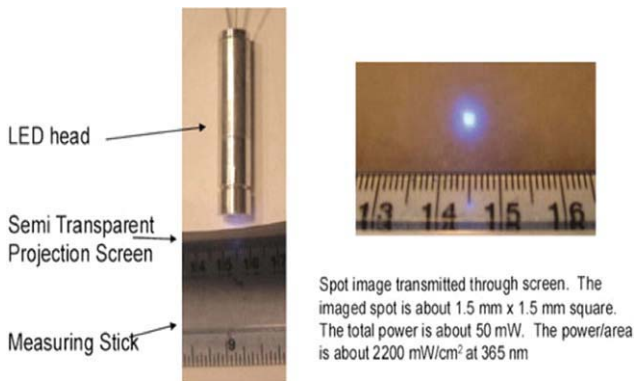

Figure 1 Compact, small-spot LED head (i.e., point LED) developed for this project by Clearstone Technologies. [Color figure can be viewed in the online issue, which is available at wileyonlinelibrary.com.]

DSC of the monomer exposed to UV light: Measuring the degree of conversion

DSC experiments

Two types of DSC experiments were conducted in this study. To determine the kinetic effects of O_2 on the photoreaction of HDDA to form polymer, a fixed volume of monomer was placed in a DSC pan and then exposed to UV radiation. The second type of DSC experiment was done on photocured inkjet-printed films. Photocuring in the DSC pans was accomplished with a small-spot UV light-emitting diode (LED) especially designed for this study (Fig. 1). Photocuring of the films was done with an LED array delivering an equivalent radiation dose. DSC analysis was performed with a TA Instruments 2910 differential scanning calorimeter. The specific methods used are considered in the following paragraphs. The various facets of the research reported here evolved in the order of presentation. As the program progressed and the influence of oxygen on photocuring became more apparent, the procedures we used were modified to mitigate the effect. Thus, there were variations in the specific experimental protocols that we followed in the different portions of the study as it evolved. Within each portion, however, the samples were treated uniformly.

To determine the degree of cure, a thermal scan was carried out on a sample previously exposed to UV light. The residual ΔH value (heat of reaction) from this was compared with a second thermal DSC scan conducted on pure HDDA monomer in an inert atmosphere. The ΔH (ΔH_s) for the residual exotherm of the photocured sample was compared to that of the unreacted pure HDDA monomer (651.5 J/g) with the following equation:

$$\left[\frac{1-\Delta H_s(\mathrm{J/g})}{651.5(\mathrm{J/g})}\right]\times 100 = \text{Conversion } (\%) \qquad (1)$$

UV curing of the DSC samples with an advanced compact LED

Photocuring in the DSC pans was accomplished with a custom-designed compact small-spot LED device from Clearstone Technologies (Minneapolis, MN), as shown in Figure 1. The LED had a square-shaped light-spot footprint of about 1.5 mm at a primary wavelength of 365 nm. The total LED power at peak was 78 mW and yielded a power/area of 3466 mW/cm^2. The dispersed halo surrounding the spot had about 1/100 of the spot power, a level that was not sufficient to effect curing. The small-spot LED gave us precise control over both the wavelength and radiation intensity delivered to the sample. It delivered light exposures of a single wavelength with uniform intensity for a controlled time interval so as to give each element exactly the same curing profile. The LED allowed for small-volume incremental light exposures, which aided stress relaxation and, thus, helped mitigate the effects of residual stresses in the films. The radiation dose imparted for curing could be adjusted by variation of the power supplied to the LED, the height of the LED above the curing monomer, and the time of exposure.

Effect of the radiation (light) dose on the conversion

The effect of the radiation dose on conversion was considered from two perspectives: (1) changes in the LED power and height above the target and (2) changes in the time of exposure. The experimental procedures used in each case are given next:

1. HDDA (5 μL, ~ 5 mg) was placed in a DSC pan. The pan was purged for 1 min under an argon blanket. After purging, the sample was exposed to UV for 1 s with various LED heights and power settings to achieve a range of dosage values (in accordance with a master LED power calibration). After curing, the samples were sealed and scanned by DSC under an N_2 atmosphere. The DSC instrument was equilibrated at 125°C and ramped at 20°C/min to 280°C.
2. HDDA (5 μL) was placed in a DSC pan. The pan was purged for 1 min under an argon blanket. The samples were exposed with the UV source at a power setting of 57.8 mW/cm^2. This setting was chosen because it allowed for a variation in the degree of conversion from 60 to 93% through changes in the exposure time. After exposure, the pans were sealed and ramped from 125 to 280°C in N_2 at 20°C/min. A series of samples was characterized with the curing time increased in 1-s intervals as a means for increasing the dosage level imparted to the samples. The dosage versus time was assumed to be an additive property. For

example, in this experiment, for a 1-s exposure, the dosage was 57.8 mJ/cm^2, and for a 2-s exposure, the dosage was 57.8 mJ/cm^2 + 57.8 mJ/cm^2 = 115.6 mJ/cm^2.

Effect of the O_2 concentration on the conversion percentage of HDDA to the polymer

The effect of atmospheric O_2 on the degree of UV photocuring was examined in this study. HDDA (5-μL samples) was placed in a DSC pan. The open pan was then placed in the DSC instrument, which was not covered. A nitrogen and air mixture circulated through the DSC cell created the atmospheric control. The small-spot LED was aligned above the sample. The cell, then, was covered with press-and-seal plastic wrap to maintain the atmospheric conditions within the cell. The DSC instrument was equilibrated and maintained at 30°C for 5 min. The LED was turned on for 1 s 1 min into the isotherm, and the resulting exotherm was measured. The sample was exposed to a dosage of 24.6 mJ/cm^2. After photocuring, the DSC was sealed, and the sample was scanned by ramping at 20°C/min to 300°C. The residual exothermic peak of HDDA during the thermal scan was used to determine the amount of reaction that occurred during UV exposure.

Inert gas purge: Time cure study

Monomer solution (5 μL) was added to a DSC pan open to the atmosphere. A number of different samples with different purge times was prepared. In each case, the pan was blanketed with argon and purged for a specific time (1, 2, 3, 4, 5, 7, 10, 15, or 30 min). The sample was cured with the small-spot LED at a power setting of 24.6 mW/cm^2. The DSC instrument was then sealed, and a scan was carried out on the sample at a heating rate of 20°C/min from ambient temperature to 300°C in an N_2 atmosphere.

Preparation and analysis of UV photocuring and conversion in the inkjet-printed films: oxygen cure study

DMA film sample preparation procedure

The films were formed by inkjet printing. The printer used was a Dimatix Materials Printer (DMP; DMP-2800) manufactured by Fujifilm-Dimatix, Inc., Santa Clara, CA. The DMP is a laboratory research printer that enables the evaluation of ink-jetting technology for new materials manufacturing and analytical processes. It is designed to carry out proof-of-concept and developmental work with sophisticated capabilities for optimizing the process parameters for a given application. The DMP is PC-controlled and has a substrate scanning ink-jet deposition system with a visual drop observation camera, spot location, and variable printing resolution. It printed with user-fillable piezo-based jetting cartridges, each with 16 nozzles at 254-μm spacing. It was designed specifically for work with organic fluid-based inks and was equipped with the capability of heating the nozzles and substrate up to 70°C.

To create film samples ready for evaluation via DMA, an ink cartridge was filled with 1.5 mL of monomer. The voltage settings on the printer were adjusted to produce 10-pL drops. A solid rectangular 4 × 1 cm^2 printing template was followed. During printing, the printer was rastered linearly from left to right and deposited enough monomer to create overlap of the drops and lines. After a single layer was printed, the entire template was covered with monomer; additional layers were then printed to add thickness to the sample.

With the DMP, 15-layer monomer films were printed that had a thickness of about 0.18 ± 0.2 mm. The substrate was a polished silicon wafer with a mirror finish. The substrate imparted a smooth, regular surface finish to the films. The mirror surface reflected light so that the incident light was reflected back through the film delivering, in effect a double light exposure to each volume element. This resulted in a more uniform cure and an increased conversion compared with a nonreflecting substrate. Two aluminum bars were placed on the wafer, and plastic shrink wrap was then applied over the wafer, film, and aluminum bars and pressed down on all sides to create a bubble over the film, which sealed in the atmosphere. The Al bars served as spacers to prevent the shrink wrap from touching the uncured film. A tube was inserted into the bubble to introduce argon gas. Next, the sample was flushed (purged) with argon for 15 min to remove all of the absorbed (dissolved) oxygen, and then, it was cured by exposure to UV light. The flow rate of the gas was maintained at a level sufficient to fill and maintain the shrink-wrap bubble. An LED array (described later) was the UV source for curing the films at a dosage of 69 mJ/cm^2 (with an exposure time of 90 s). It was placed directly over the shrink wrap, and the sample was exposed through the shrink-wrap covering. After curing, the films were removed from the silicon wafer and characterized by DSC and DMA

UV curing of the films with an LED array

Photocuring of films was accomplished with an LED array LH365-B device from Clearstone Technologies, which delivered a nominal intensity of 210 mW/cm^2. The device consisted of an array of 18 LEDs,

which covered an area of 20 cm^2. For DSC analyses of the films, about 10 mg of the cured film was placed in a standard DSC pan and ramped at 20°C/min to 300°C. The data showed that the inkjet-printed films were generally cured to approximately 93% conversion.

DMA characterization of the films

DMA measurements of the viscoelastic properties were performed on film specimens in a constant-frequency-ramped temperature tensile mode. The DMA samples were subjected to a small-amplitude oscillating strain (or vibration) at a fixed frequency. The storage modulus and tan δ data were recorded. The storage modulus is related to the energy stored during the deformation and reflects the solidlike character or elastic stiffness of the material. Tan δ is related to the ability of a material to dissipate or dampen mechanical energy.

DMA analysis was performed with a TA Instruments Q800 dynamic mechanical analyzer in the tensile mode with a thin-film sample fixture. The following parameters were used for testing: the strain amplitude was 5 μm, a preload force of 0.0100 N was used, the force track was 110%, the frequency was 1 Hz, and the temperature ramp rate was 3°C/min. The DMA samples were rectangular. The sample dimensions varied from 12 to18 mm (x) × 7 to 10 mm (y) × 0.25 to 0.50 mm (z). We controlled the atmosphere by placing a gas inlet tube inside the top of the DMA oven. The gases (air and nitrogen) were mixed before introduction into the DMA at a fixed flow rate. Both the first and second runs of the films were carried out under identical atmospheric conditions to maintain consistency. After the first scan, the samples were unclamped on one end and allowed to cool to room temperature. Then, they were reclamped, and the second run was performed.

The DMA measurement procedure was as follows:

1. Equilibration was carried out at 30°C (this started every sample at the same temperature).
2. The oven was held isothermally for 2 min (this allowed the oven to fill with gas to vary the atmosphere).
3. Data collection was then started.
4. The sample temperature was ramped at 3°C/min to 200°C.

RESULTS AND DISCUSSION

Double-bond conversion versus the UV dosage

The reaction conversion versus the UV light dosage data in Figure 2 indicate the general form of the conversion/dosage profiles. Also shown in Figure 2 is the difference in conversion achieved when the reaction was carried out with and without O_2 inhibition. The curve denoted by diamonds represents the conversion/dosage profile after the monomer was purged with an inert atmosphere for 1 min; squares represent the conversion/dosage profile after the monomer was purged with an inert atmosphere for 15 min. The 15-min time period was selected from the experimental purge time cure study data (presented later in Fig. 7). Clearly, gelation and vitrification in this system occurred at low UV dosages and relatively short times when oxygen was excluded. These data were generated by the variation of the UV dosage by changes in the UV light power intensity and height of the UV source above the sample.

The corresponding data shown in Figure 3 for samples purged in an inert atmosphere for 1 min were obtained by the increase of the exposure time in 1-s increments at a constant LED power setting of 24.6 mW/cm^2. A comparison of the two curves from Figures 2 and 3, as shown in Figure 4, indicated that the higher dosage exposure over a short time period yielded a greater degree of conversion than a lower dosage over a long time period. This resulted from the combination of a higher free-radical concentration in the case of greater light intensity, which more quickly overcame the effect of absorbed O_2, and higher localized temperatures,[37,38] which developed because of a greater heat release rate.

Effect of oxygen on the photoreaction

Figure 5 shows the effects on conversion when photocuring was done in an atmosphere with various

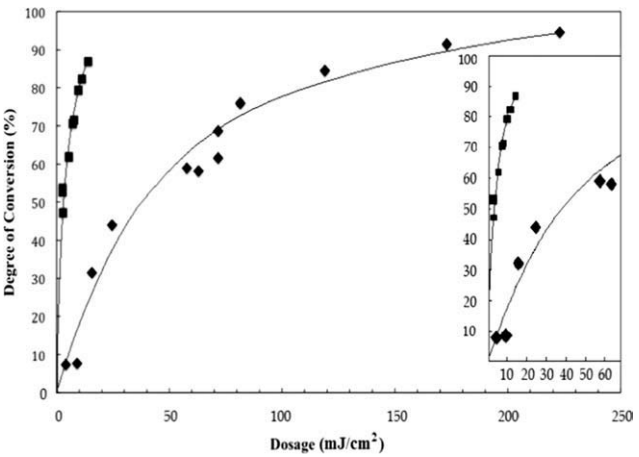

Figure 2 Relationship between the degree of conversion of HDDA (cure percentage) and the UV light dosage: conversion/dosage profile after the purging of the monomer with an inert atmosphere for (◆) 1 min before UV exposure and (■) 15 min. The UV dosage was increased by an increase in the power delivered by the LED light source or in the height of the source above the sample.

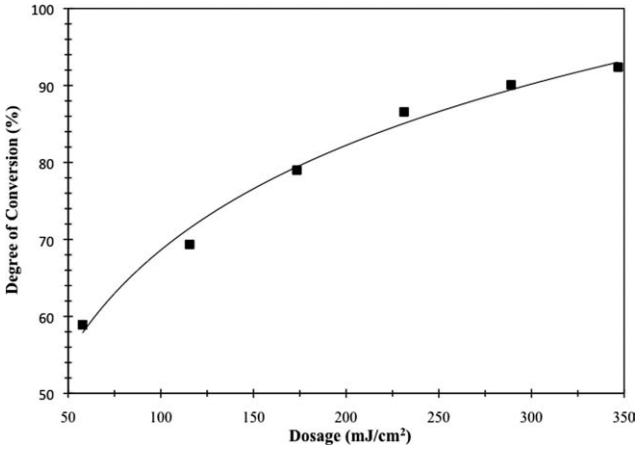

Figure 3 Relationship between the conversion of HDDA (cure percentage) and UV light dosage delivered due to increasing the time of exposure (in 1-s increments); the inert gas purge time was 1 min before UV exposure.

concentrations of O_2, ranging from inert gas (0% O_2) to that of air (21% O_2). As the O_2 concentration increased, the conversion achieved for a given radiation dose diminished significantly. Samples were purged in an ambient atmosphere for 1 min before UV exposure. This demonstrated the importance of the oxygen concentration on the photoreaction process. It also emphasized the importance of implementing an inert gas atmosphere in the formation of films by photocuring in layered manufacturing via inkjet printing. We observed that without an inert atmosphere, the inkjet-printed films cured only partially and were nonuniform, with a surface layer of uncured monomer remaining. This illustrated the

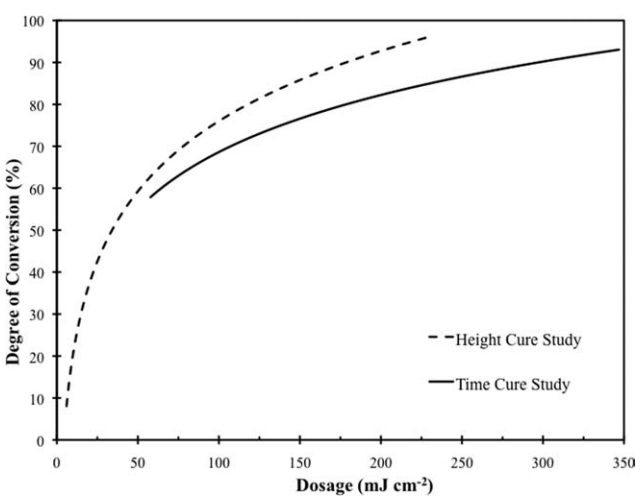

Figure 4 Relationship between the dosage obtained by changing UV source height and power (or intensity; Fig. 2) and increasing exposure time at a constant power setting (Fig. 3). These curves were calculated from the data of Figures 2 and 3 for samples purged with an inert atmosphere for 1 min before light exposure.

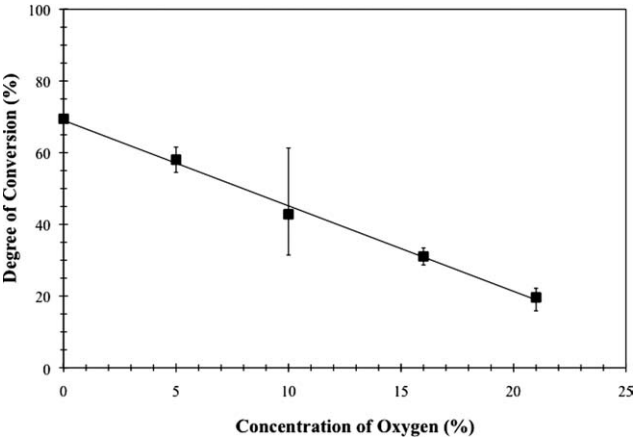

Figure 5 Effect of the O_2 concentration in the atmosphere on the degree of conversion (each data point is based on the average of five experimental DSC scans).

idea that dissolved oxygen markedly increased the gelation dose, the amount of radiation required to cause gelation.

The DSC data indicating the thermal postcuring exotherms that were observed for these samples are shown as an overlay in Figure 6. The general trend of the exotherms shifting to higher temperatures and diminishing in intensity with decreasing O_2 concentration was consistent with decreasing molecular mobility in the system as the crosslink density increased from photocuring. Higher temperatures had to be reached as the crosslink density increased for the residual monomer to diffuse and react.

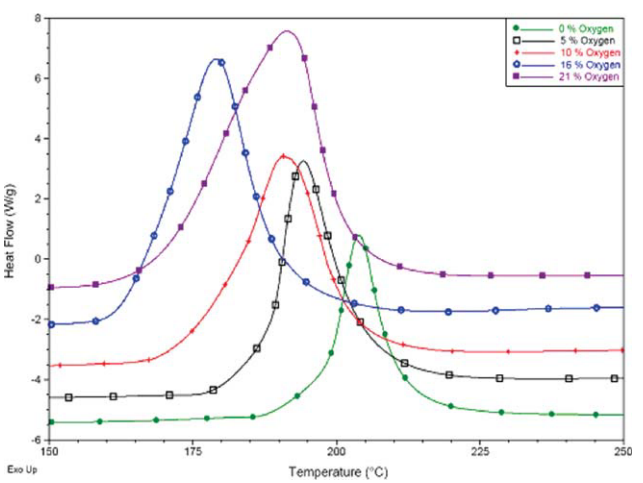

Figure 6 DSC thermal scans showing residual reaction exotherms for various photocured samples from the atmosphere variation cure study (heating rate = 20°C/min from 30 to 250°C in an N_2 atmosphere). The magnitudes and positions of the exotherms were influenced by different degrees of oxygen inhibition during the photopolymerization. (Baselines for the individual curves were shifted to improve the clarity of the data presentation.) [Color figure can be viewed in the online issue, which is available at wileyonlinelibrary.com.]

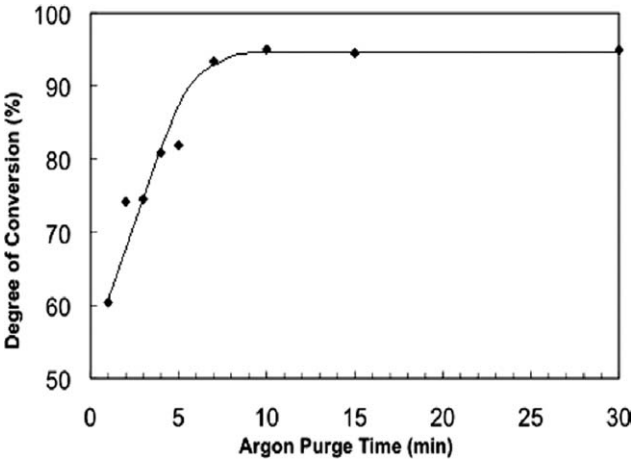

Figure 7 Inert gas purge time cure study with exposure of HDDA to an argon atmosphere showing the relationship between the percentage conversion and the purge time in argon.

Purge time cure study of HDDA in argon

The data of Figure 7 indicate the effect of the purging of samples with an inert atmosphere for various times to cause oxygen to diffuse out of the samples. By integrating the exotherm associated with the thermal postcuring of the partially cured HDDA sample to yield a residual ΔH_s and relating it to the ΔH_R (heat of reaction of unreacted monomer) for thermal curing of the unreacted monomer, we obtained a percentage conversion for each sample. After 10 min of purging, the percentage conversion achieved was about 95% and had leveled off. As a result, we chose the consistent purge time of 15 min as a conservative value for the exposure of films prepared for mechanical, DMA studies. This conservative purge time value was chosen to negate the effects of any residual oxygen absorbed into the monomer. The data of Figure 7, including ΔH values, are listed in Table I.

DMA data for the inkjet-printed films

Film samples were cured under identical conditions but were exposed to various O_2 concentrations during the DMA variable temperature scans. Two DMA scans were completed for each sample. After a first scan was completed, each sample was cooled to room temperature, and a second scan was performed immediately afterward. The first-scan data are shown in Figure 8. The degrees of conversion and modulus values for these samples were similar before the DMA scans began. After the first DMA scan, the modulus curves shifted upward slightly. The upward shift was indicative of both the crosslinking density increasing somewhat and the residual monomer content decreasing. However, the plateau modulus values above the glass transition were directly related to the O_2 concentration in the DMA oven during the test. The DMA data for the second scans for the same samples are shown in Figure 9(a,b), which shows the storage modulus and tan δ data for film samples exposed to different O_2 levels during the first DMA scans. Again, the modulus values at 200°C were proportional to the O_2 atmospheric concentration in the DMA oven (see also Fig. 13, shown later). The data in Figure 10 show this more clearly. They also indicate that the plateau modulus values (above T_g) were the same after the end of both the first and second scans. Thus, after the first scan, conversion was virtually complete, and the final crosslinking network was established.

Thus, the DMA data indicated that the degree of crosslinking achieved during the thermal postcuring, which occurred as the sample was first heated up to 200°C, was related to the amount of O_2 present in the DMA atmosphere. The source of oxygen entering the films was diffusion from the surrounding atmosphere. From the observed changes in the plateau

TABLE I
Residual Heat of Reaction Data from the DSC Scans of Samples with Various Argon Purge Times Cured with the Point LED at a Height of 1 in., a Power Setting of 100%, and a Total Radiation Dose of 24.6 mJ/cm^2

Purge time (min)	ΔH_s (J/G)	Conversion (%)
1.0	253.9	60.4
3.0	163.5	74.5
5.0	116.0	81.9
7.0	41.7	93.4
10.0	31.9	95.0
15.0	35.0	94.5
30.0	32.3	95.0

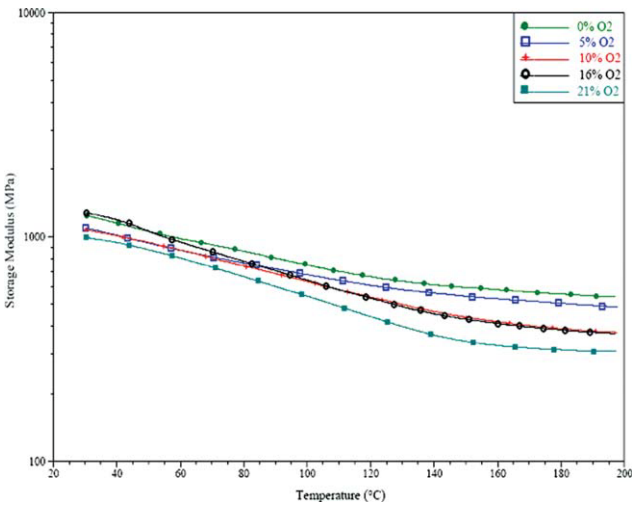

Figure 8 DMA first scans: DMA data for the storage moduli of film samples cured under identical conditions in argon but exposed to various O_2 concentrations during the DMA temperature scans. [Color figure can be viewed in the online issue, which is available at wileyonlinelibrary.com.]

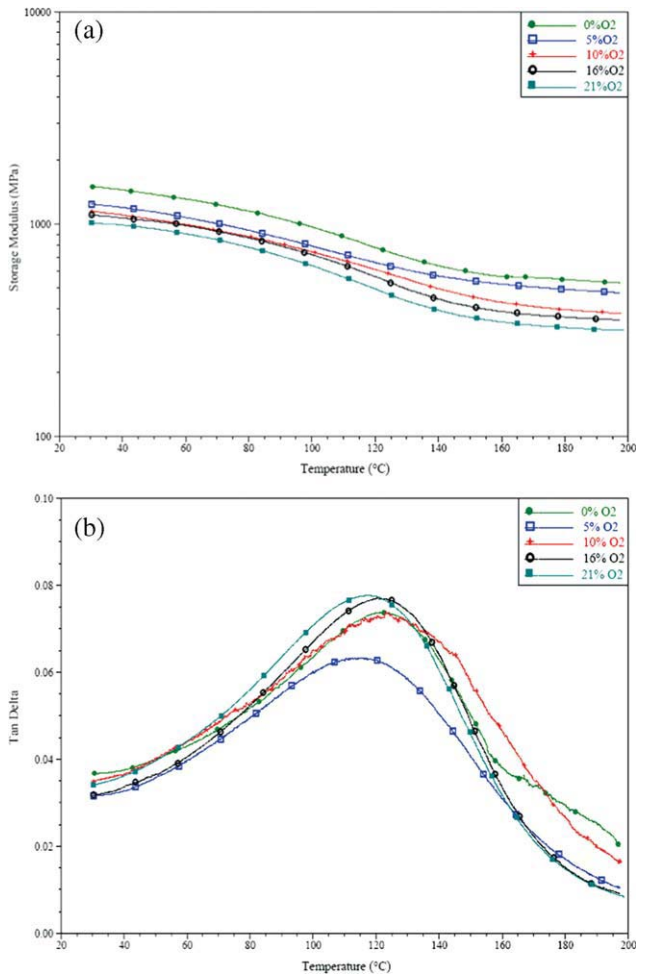

Figure 9 (a) DMA second-scan data for the storage moduli of the film samples cured under identical conditions in argon but exposed to various O_2 concentrations during the DMA temperature scans; these data are the second scans for the same samples shown in Figure 8. (b) Tan δ curves for the second-scan DMA data shown in part a. [Color figure can be viewed in the online issue, which is available at wileyonlinelibrary.com.]

modulus values, it was apparent that oxygen reduced the crosslinking density of the network formed. This may have occurred (1) as a result of network chain extension via the reaction of residual monomer with dangling acrylate double bonds from the monomer units already incorporated into the network during the initial photoreaction; (2) because of a reduction in the kinetic chain length during the thermal polymerization due to O_2, which opened up the network because of the addition of more chain ends;[9] or (3) both.

We noted in the Introduction section that if oxygen is present, an induction time will be observed because the polymerization cannot proceed until the propagation reaction competes favorably with the inhibition reaction. In thicker films, the lower depths of the film may polymerize, whereas the top layer remains liquid or tacky because oxygen inhibits the surface reaction.[12,13] An example of this effect in the DMA data is illustrated in Figure 11 for a film prepared in air and then exposed to air during the DMA scan. Initially, the film was rubbery and had a liquid layer on the surface. The storage modulus data for this sample [Fig. 11(a)] indicated that this partially cured sample (scan 1) thermally crosslinked during the DMA scan. The modulus first decreased at the T_g of the partially cured sample and then increased. This resulted in a higher modulus in scan 2, which changed little in scan 3.

Figure 11(b) shows the tan δ curves for the same film sample cured in air. The peak tan δ temperature (taken as T_g) increased considerably from scan 1 to scan 2. It was apparent that the partially crosslinked polymer containing considerable unreacted monomer was converted during scan 1 to a more highly crosslinked material with a T_g almost 40°C higher. The crosslinking reaction during DMA scan 1 occurred in two stages, as indicated by the double rise in modulus that was apparent in the data. This was likely due to an interplay between the reaction kinetics and viscoelasticity observed in the nonisothermal curing of thermosets, which has been referred to as *kinetic viscoelasticity*.[39–41]

The results obtained by the completion of a DSC simulation of the same reaction sequence were consistent with this. HDDA was cured in a DSC pan with the same procedure as followed for the DMA sample shown in Figure 11. After the initial photoreaction in air, the degree of conversion was around 70%, with unreacted monomer still on the surface. A thermal DSC scan then was performed on the

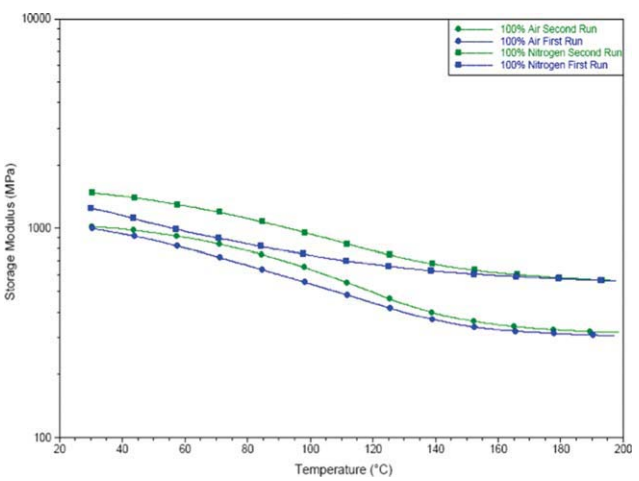

Figure 10 Comparison of the DMA scans for films illustrating the differences between the first scan and second scan for the extremes in the oxygen exposure study. The 100% air sample and the 100% nitrogen sample represented the greatest differences in O_2 exposure during the thermal postcuring that occurred during the DMA tests. [Color figure can be viewed in the online issue, which is available at wileyonlinelibrary.com.]

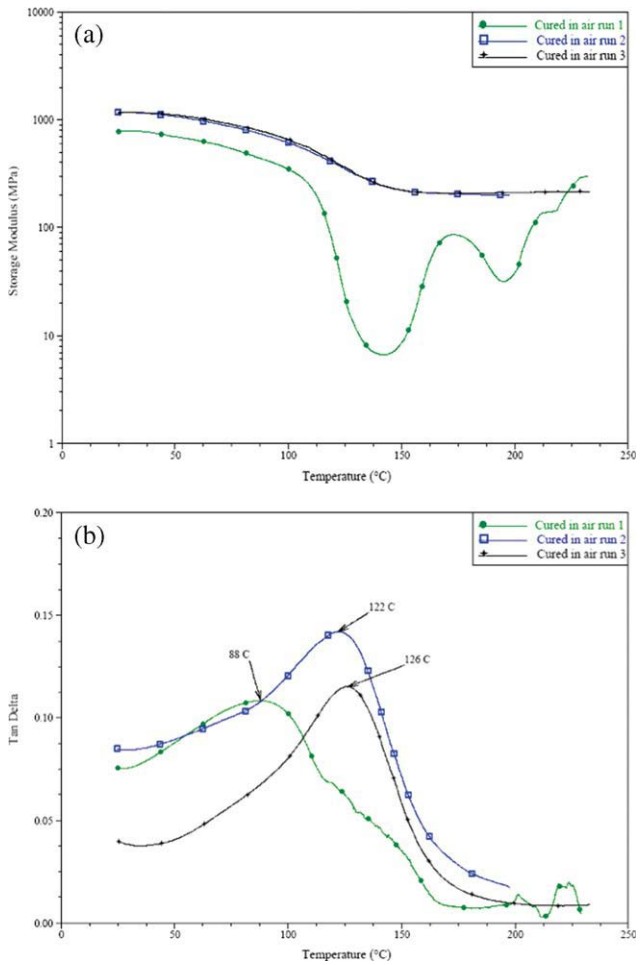

Figure 11 (a) Storage modulus curves for the film sample cured by UV light in air: sequence of three DMA scans run sequentially, which shows that the partially cured sample (run 1) thermally crosslinked during the DMA scan. This resulted in a higher modulus in scan 2, which changed little in scan 3. (b) Tan δ curves for the same film sample cured in air; the temperatures for the peaks (taken as T_g) increased considerably from scan 1 to scan 2. [Color figure can be viewed in the online issue, which is available at wileyonlinelibrary.wiley.com.]

photocured DSC sample. Two distinct exothermic events were observed, one covering the range 50–115°C and a second covering the range from 140 to 210°C. The lower temperature event most likely arose both from the reaction of residual monomer with trapped radicals and dangling acrylate groups tied to the crosslinking network and with residual monomer. These reactions became viable above the initial T_g when mobility in the network was sufficient to facilitate the diffusion of the monomer. Dangling acrylate groups arising from monomer units already attached to a network are expected to have increased thermal reactivity.[28–31] A reaction in this region will continue until vitrification occurs because of crosslink network buildup. At the same time, the radical population also will be diminished. At higher

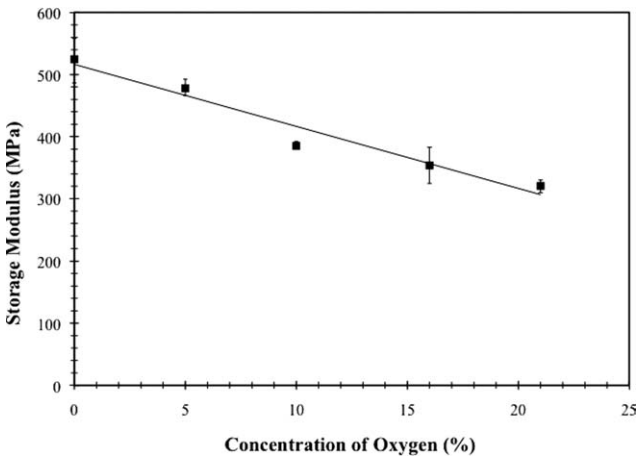

Figure 12 Storage modulus values at 200°C versus the concentration of O_2 (O_2 percentage) in the DMA oven during measurement; the modulus values were recorded after the second scans such as those shown in Figure 9a (each data point is based on the average of five experimental trials).

temperatures, devitrification will occur, and additional radicals will be generated by thermal activation. The higher temperature exotherm occurred in the temperature range where neat, unreacted HDDA is known to undergo polymerization.

Figure 12 represents the 200°C storage modulus values for samples exposed to a given N_2 concentration during the DMA scan; modulus values were taken at 200°C, near the end of the second scan. The data indicated that the exposure to various amounts of O_2 during curing resulted in a linear trend, which was representative of the differences in the crosslinking density, which resulted from exposure to O_2. The T_g values for this system varied only slightly over the range of O_2 concentrations. However, there

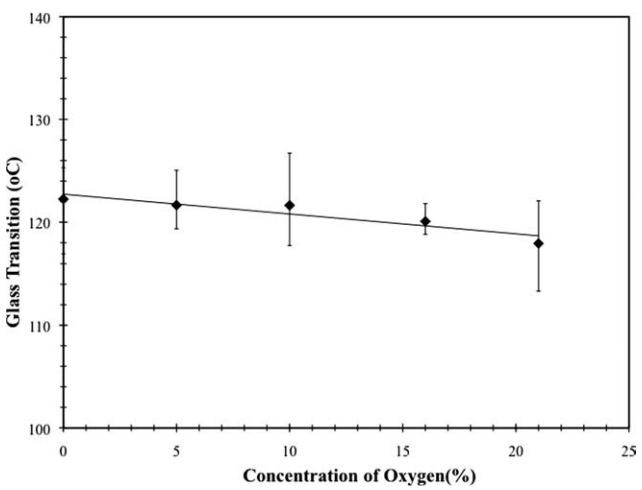

Figure 13 T_g values from the second-scan DMA data taken from peaks in the tan δ curves similar to those shown in Figure 9(b) (each data point is based on the average of five experimental trials).

was a linear trend of decreasing T_g values with increasing O_2 concentration, as indicated in Figure 13. This was consistent with the apparent decrease in the crosslink density suggested by the corresponding decrease in plateau modulus values.

CONCLUSIONS

The objective of this study was to obtain data relevant to the formation of viable crosslinked films of HDDA by photoreaction in a layered manufacturing inkjet-printing process. The influence of atmospheric oxygen on the photoreaction of HDDA to form crosslinked polymers was investigated with thermal analysis to characterize the effects of various O_2 concentrations on both the photocuring and the subsequent dark reaction. Photocuring was achieved with UV LED light sources emitting at 365 nm. Atmospheric oxygen had a pronounced effect on the rate of photoreaction of HDDA and on the crosslinking that occurred both during photocuring and in the dark during subsequent thermal postcuring. Exposure to increasing amounts of O_2 during the photocuring severely restricted the degree of conversion and the UV dose required for gelation in proportion to the O_2 concentration. The initial exposure to O_2 also affected the rate and temperature range of thermal postcuring.

We determined that inkjet-printed HDDA films picked up considerable absorbed O_2 during printing so that even in an inert atmosphere, inkjet-printed HDDA films did not cure easily unless they were first purged with an inert gas to desorb O_2. Thus, printed films of HDDA were difficult to cure in air, with normal UV radiation dose levels; this resulted in film specimens that were rubbery, with liquid monomer on the surface. Using DSC samples as test specimens, we found that after a 10-min purge with an inert gas, HDDA reacted to over 90% conversion with modest UV dose rates. However, some residual double-bond concentration generally remained after UV exposure. On the basis of this, as a conservative measure, the process for printing films was modified to include purging in an inert atmosphere for 15 min before photocuring.

The viscoelastic properties of the photocured films were characterized by DMA. Additional crosslinking proceeded after the photoreaction, in the dark, during DMA scans at temperatures above T_g. This was due to the reaction of trapped free radicals with residual monomer and by the thermal initiation of monomer to form additional network chains. We found that the concentration of O_2 surrounding the sample influenced the viscoelastic property data measured during variable-temperature DMA scans. The nature of the differences indicated that the presence of oxygen affected the crosslinking that occurred during this postcuring or dark reaction process. The final crosslink density was greater in the fully cured DMA samples that were exposed to atmospheres with increasing inert gas concentrations. The viscoelastic property data indicated that exposure to reduced oxygen concentrations during thermal postcuring in the DMA resulted in a linear trend of increasing plateau modulus above T_g and increasing T_g itself. The fact that the O_2 concentration in the atmosphere surrounding DMA samples affected their final mechanical properties indicated that the diffusion of O_2 into the films was an important factor in determining their crosslink densities.

References

1. Decker, C. Acta Polym 1994, 45, 333.
2. Decker, C. J Coat Technol 1987, 59, 97.
3. Odian, G. Principles of Polymerization; Wiley: New York, 1991; p 768.
4. Decker, C. Makromol Chem Macromol Chem Phys 1979, 180, 2027.
5. Decker, C.; Faure, J.; Fizet, M.; Rychla, L. Photogr Sci Eng 1979, 23, 137.
6. Decker, C.; Jenkins, A. D. Macromolecules 1985, 18, 1241.
7. Miller, C. W.; Hoyler, C. E.; Jonssen, S.; Nason, C.; Lee, T. Y.; Kuang, W. F.Viswanathan, K. *N*-Vinylamides and Reduction of Oxygen Inhibition in Photopolymerization of Simple Acrylate Formulations; American Chemical Society: Washington, DC, 2003; p 1.
8. Krongauz, V. V.; Chawla, C. P.; Dupre, J. Oxygen and Radical Photopolymerization in Film; American Chemical Society: Washington, DC, 2003; p 1.
9. Lovell, L. G.; Bowman, C. N. Polymer 2003, 44, 39.
10. Berchtold, K. A.; Lovell, L. G.; Nie, J.; Hacioglu, B.; Bowman, C. N. Polymer 2001, 42, 4925.
11. Berchtold, K. A.; Lovell, L. G.; Nie, J.; Hacioglu, B.; Bowman, C. N. Macromolecules 2001, 34, 103.
12. Gou, L.; Corestsopoulous, N.; Scranton, A. B. J Polym Sci Part A: Polym Chem 2003, 42, 1285.
13. Cao, L. H.; Currie, E.; Tilley, M.; Jean, Y. C. In "Photoinitiated Polymerization"; ACS Symposium Series 847, Belfield, K. D.; Crivello, J. V., Eds.; American Chemical Society, Columbus, OH (2003).
14. Decker, C.; Moussa, K. Makromol Chem Macromol Chem Phys 1988, 189, 2381.
15. Krongauz, V. V.; Schmelzer, E. R. Polymer 1992, 33, 1893.
16. Decker, C. Macromolecules 1989, 22, 12.
17. Decker, C.; Moussa, K. Makromol Chem Macromol Chem Phys 1990, 191, 963.
18. Nunes, T. G.; Ceballos, L.; Osorio, R.; Toledano, M. Biomaterials 2005, 26, 1809.
19. Pereira, S. G.; Reis, N.; Nunes, T. G. Polymer 2005, 46, 8034.
20. Chong, J. S. J Appl Polym Sci 1969, 13, 241.
21. Dickey, M. D.; Burns, R. L.; Kim, E. K.; Johnson, S. C.; Stacey, N. A.; Willson, C. G. AIChE J 2005, 51, 2547.
22. Brady, G. A.; Halloran, J. W. J Mater Sci 1998, 33, 4551.
23. Espanet, A.; Ecoffet, C.; Lougnot, D. J. J Polym Sci Part A: Polym Chem 1999, 37, 2075.
24. Andrzejewska, E.; Bogacki, M. B.; Andrzejewski, M.; Janaszczyk, M. Phys Chem Chem Phys 2003, 5, 2635.
25. Korolev, G. V.; Mogilevich, M. M. Three-Dimensional Free-Radical Polymerization: Cross-Linked and Hyper-Branched Polymers; Springer-Verlag: Berlin, 2009.
26. O'Brien, A. K.; Bowman, C. N. Macromolecules 2006, 39, 2501–2506.

27. Chartoff, R. P. J Therm Anal Calorim 2006, 85, 213.
28. Kloosterboer, J. G. Makromol Chem Makromol Symp 1989, 224, 223.
29. Boots, H. M. J.; Kloosterboer, J. G.; Van de Hei, G. M. M.; Pandey, R. B. Br Polym J 1985, 17, 219.
30. Kloosterboer, J. G.; Lijten, G. F. C. M.; Boots, H. M. J Makromol Chem Macromol Symp 1989, 24, 223.
31. Kloosterboer, J. G.; Lijten, G. F. C. M.; Zegers, C. P. G. Am Chem Soc Polym Mater Sci Eng Prepr 1989, 60, 122.
32. Chartoff, R.; McMorrow, B. In Proceedings of the 32nd NATAS Conference, Williamsburg, VA, Oct 2004.
33. Krongauz, V. V.; Chawla, C. P., J.; Dupre, J. Oxygen and Radical Photopolymerization in Film; American Chemical Society: Washington, DC, 2003; p 1.
34. Studer, K.; Decker, C.; Beck, E.; Schwalm, R. Prog Org Coat 2003, 48, 92.
35. Studer, K.; Decker, C.; Beck, E.; Schwalm, R. Prog Org Coat 2003, 48, 101.
36. Weissman, P.; Chartoff, R.; Linden, S.-M. In Proceedings of the 20th North American Thermal Analysis Society Conference, Minneapolis, MN, Sept 1991.
37. Flach, L.; Chartoff, R. Polym Eng Sci 1995, 35, 483.
38. Flach, L.; Chartoff, R. Polym Eng Sci 1995, 35, 493.
39. Dillman, S. H. Ph.D. dissertation, University of Washington, 1988.
40. Dillman, S. H.; Seferis, J. C. J Macromol Sci Chem 1989, 26, 227.
41. Chartoff, R.; Mengzel, J.; Dillman, S. In Thermal Analysis of Polymers: Fundamentals and Applications; Mengzel, J.; Prime, R. B., Eds.; Wiley: New York, 2009; Chapter 5.